

AD-A145 606 KINETICS OF SIMPLE INNER- AND OUTER-SPHERE  
LAFAYETTE IN DEPT OF CHEMISTRY S FARQUHARSON ET AL.  
UNCLASSIFIED SEP 84 TR-35 N00014-79-C-0670 F/G 7/4

KINETICS OF SIMPLE INNER- AND OUTER-SPHERE  
ELECTROCHEMICAL REACTIONS AT R. (U) PURDUE UNIV  
LAFAYETTE IN DEPT OF CHEMISTRY S FARQUHARSON ET AL.  
SEP 84 TR-35 N00014-79-C-0670 F/G 7/4

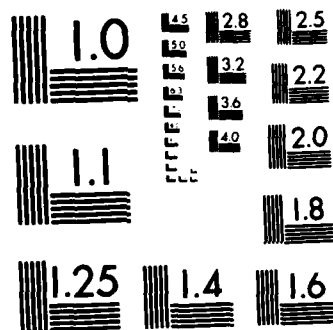
NL

[illegible]

END

## REFERENCES

DTM



MICROCOPY RESOLUTION TEST CHART  
NATIONAL BUREAU OF STANDARDS-1963-A

OFFICE OF NAVAL RESEARCH

Contract N00014-79-C-0670

TECHNICAL REPORT NO. 35

Kinetics of Simple Inner- and Outer-Sphere  
Electrochemical Reactions at Rotating Silver  
Electrodes as Examined using Surface-Enhanced  
Raman Spectroscopy

by

S. Farquharson, D. Milner, M. A. Tadayyoni

and M. J. Weaver

Prepared for Publication

in the

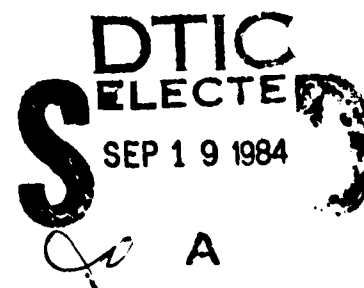
Journal of Electroanalytical Chemistry

Department of Chemistry

Purdue University

West Lafayette, IN 47907

September 1984



Reproduction in whole or in part is permitted for  
any purpose of the United States Government

This document has been approved for public release  
and sale; its distribution is unlimited

AD-A145 606

DTIC FILE COPY

84 09 18 248

REPORT DOCUMENTATION PAGE		READ INSTRUCTIONS BEFORE COMPLETING FORM
1. REPORT NUMBER Technical Report No. 35	2. GOVT ACCESSION NO. <b>A145606</b>	3. RECIPIENT'S CATALOG NUMBER
4. TITLE (and Subtitle) Kinetics of Simple Inner- and Outer-Sphere Electrochemical Reactions at Rotating Silver Electrodes as Examined using Surface-Enhanced Raman Spectroscopy		5. TYPE OF REPORT & PERIOD COVERED Technical Report No. 34
7. AUTHOR(s) S. Farquharson, D. Milner, M. A. Tadayyoni and M. J. Weaver		6. PERFORMING ORG. REPORT NUMBER
9. PERFORMING ORGANIZATION NAME AND ADDRESS Department of Chemistry Purdue University West Lafayette, Indiana 47907		8. CONTRACT OR GRANT NUMBER(s) N00014-79-C-0670
11. CONTROLLING OFFICE NAME AND ADDRESS Office of Naval Research Department of the Navy Arlington, VA 22217		10. PROGRAM ELEMENT, PROJECT, TASK AREA & WORK UNIT NUMBERS
14. MONITORING AGENCY NAME & ADDRESS (if different from Controlling Office)		12. REPORT DATE September 1984
		13. NUMBER OF PAGES
		15. SECURITY CLASS. (of this report)  Unclassified
		15a. DECLASSIFICATION DOWNGRADING SCHEDULE
16. DISTRIBUTION STATEMENT (of this Report)  Approved for Public Release; distribution unlimited		
17. DISTRIBUTION STATEMENT (of the abstract entered in Block 20, if different from Report)		
18. SUPPLEMENTARY NOTES		
19. KEY WORDS (Continue on reverse side if necessary and identify by block number)  SERS; rotating disk electrode; kinetic behavior; faradaic current flow		
20. ABSTRACT (Continue on reverse side if necessary and identify by block number) An application of surface-enhanced Raman spectroscopy (SERS) to evaluating the kinetics of electrochemical reactions is outlined. This involves monitoring the potential-dependent SERS intensities of the adsorbed reactant at a rotating disk electrode in a potential region where the kinetics are under mixed mass transfer-heterogeneous electron transfer control. Comparisons are made between the kinetic behavior extracted from the SERS intensity-potential dependence and that obtained from the faradaic current flow. For $\text{Co}(\text{NH}_3)_6^{3+}$ reduction at silver, where the reactant is electrostatically		

attracted but not bound to the surface, the SERS and electrochemical rate behavior is closely compatible. However, for  $\text{Cr}(\text{NH}_3)_5\text{Br}^{2+}$  and  $\text{Cr}(\text{NH}_3)_5\text{NCS}^{2+}$  reduction, where the reactants bind directly to the surface prior to electron transfer, the reactivities at the SERS-active sites are substantially higher than for the prevalent adsorbate as obtained electrochemically. These findings suggest that surface sites displaying efficient Raman scattering may also provide centers of catalytic activity.

attracted but not bound to the surface, the SERS and electrochemical rate behavior is closely compatible. However, for  $\text{Cr}(\text{NH}_3)_5\text{Br}^{2+}$  and  $\text{Cr}(\text{NH}_3)_5\text{NCS}^{2+}$  reduction, where the reactants bind directly to the surface prior to electron transfer, the reactivities at the SERS-active sites are substantially higher than for the prevalent adsorbate as obtained electrochemically. These findings suggest that surface sites displaying efficient Raman scattering may also provide centers of catalytic activity.

OTIC  
COPY  
INSP...

NY Letter For  
Mr. [redacted]  
Room 135  
Washington D.  
Justified

[redacted]

[redacted] +8

A1

A1

## A1

An application of surface-enhanced Raman spectroscopy (SERS) to evaluating the kinetics of electrochemical reactions is outlined. This involves monitoring the potential-dependent SERS intensities of the adsorbed reactant at a rotating disk electrode in a potential region where the kinetics are under mixed mass transfer-heterogeneous electron transfer control. Comparisons are made between the kinetic behavior extracted from the SERS intensity-potential dependence and that obtained from the faradaic current flow. For  $\text{Co}(\text{NH}_3)_6^{3+}$  reduction at silver, where the reactant is electrostatically attracted but not bound to the surface, the SERS and electrochemical rate behavior is closely compatible. However, for  $\text{Cr}(\text{NH}_3)_5\text{Br}^{2+}$  and  $\text{Cr}(\text{NH}_3)_5\text{NCS}^{2+}$  reduction, where the reactants bind directly to the surface prior to electron transfer, the reactivities at the SERS-active sites are substantially higher than for the prevalent adsorbate as obtained electrochemically. These findings suggest that surface sites displaying efficient Raman scattering may also provide centers of catalytic activity.

\*Author to whom correspondence should be addressed.

It is now well established that a variety of species when adsorbed on certain metal surfaces, most prominently silver, gold, and copper, can yield easily detectable Raman spectra as a result of surface-enhanced Raman scattering (SERS).<sup>1</sup> This *in situ* spectroscopic technique is especially applicable to electrochemical systems; Raman signals arising entirely from interfacial species can be obtained using conventional cell configurations even in the presence of substantial bulk concentrations ( $\leq 0.1$  M) of the Raman scatterer. Although considerable application to the molecular characterization of metal-solution interfaces is envisaged, such developments are still in their infancy.

A key issue to be addressed in the application of SERS to surface electrochemistry is the correspondence between the properties of the adsorbate molecules that contribute predominantly to the spectral signals and those which are primarily responsible for the observed electrochemical behavior, such as faradaic current flow. This issue is somewhat clouded by the likelihood that the sites responsible for SERS constitute only a small minority of the overall surface. These sites may be associated with metal clusters or other surface morphologies.<sup>2</sup> Thus the viability of SERS as a surface electrochemical technique hinges on the correlation, if any, between the chemical properties of the SERS-active species and those of the overall adsorbate. However, surprisingly few such comparisons have been reported.<sup>3-7</sup> The present communication describes some preliminary evaluations of the electroreduction kinetics of adsorbed species using SERS, and the comparison with the kinetics as determined from faradaic current flow. These experiments appear to be the first application of SERS to electron-transfer dynamics at metal surfaces.

We have recently been examining surface-enhanced Raman (SER) spectra for a variety of simple inorganic adsorbates at the silver-aqueous interface under conditions where the surface composition can be characterized by independent means.<sup>3-8</sup> These include substitutionally inert transition-metal complexes, especially Co(III), Cr(III), Ru(III), and Os(III) ~~ammines~~ amines, whose surface concentrations can be obtained in favorable cases from the charge required to reduce the metal cation as measured using electrochemical perturbation techniques.<sup>9,10</sup> Suitably intense SER spectra can be obtained for a number of such couples that are bound to the surface via bridging ligands, notably bromide, thiocyanate, or pyrazine. We have also observed that SER spectra can be obtained at silver for *unbound* molecules, most notably metal hexaammine cations, when they are electrostatically attracted into the diffuse layer<sup>7</sup> (*vide infra*).

The occurrence of electron-transfer reactions involving such interfacial species can readily be detected using SERS since several features of the Raman spectra, including vibrational frequencies, are sensitive to the metal oxidation state. Redox thermodynamic data have been obtained from potential-dependent SER spectra for several adsorbed Ru(III)/(II) and Os(III)/(II) couples.<sup>6,7</sup> These data are in good agreement (surface formal potentials within ca 20 mV) with the corresponding information obtained from conventional electrochemistry.<sup>6,7</sup>

These recent findings regarding redox equilibria have led us to consider ways in which SERS can be utilized to probe the redox *reactivity* of molecules at metal surfaces. Two general approaches can be envisaged. The first involves monitoring the time dependence of the adsorbed reactant (or product) concentration in response to a rapid electrochemical perturbation. Such experiments are feasible using an array detector system as employed in our laboratory (PAR OMA-2).

However, the experiments reported here employ a simpler approach, involving monitoring the SER spectra at a rotating disk electrode as a function of potential. Cobalt(III) and chromium(III) reactants were chosen that exhibit totally irreversible electroreductions at silver electrodes under these conditions. In other words, the rotating disk voltammograms for these systems are controlled by the heterogeneous electron-transfer kinetics along with mass transport of the reactant to the electrode surface. This leads to the following analysis.

The reactant concentration close to the electrode surface,  $C_s$ , (i.e. the three-dimensional concentration just outside the double layer) will progressively decrease relative to the bulk concentration,  $C_b$ , on the rising part of the voltammetric wave according to<sup>11,12</sup>

$$C_s = C_b [(i_l - i)/i_l] \quad (1)$$

where  $i$  is the current density at a given potential, and  $i_l$  is the mass transport-limited current density. The integrated intensity of a given Raman band for an adsorbed species,  $I_{SER}$ , is expected to be roughly proportional to its (two-dimensional) surface concentration,  $\Gamma_s$ , at the SERS-active surface sites. As the reaction rate at these sites increases, the steady-state value of  $\Gamma_s$  and hence  $I_{SER}$  will decrease. Provided that the reactivity of the SERS-active adsorbate does not differ from that associated with the remaining surface sites, these decreases in  $\Gamma_s$  will occur uniformly across the surface. If  $\Gamma_s$  is in turn proportional to  $C_s$  (i.e. Henry's Law applies) then

$$I_{SER} = I_{SER}^0 [(i_l - i)/i_l] \quad (2)$$

4

The quantity  $I_{SER}^c$  is the value of  $I_{SER}$  that would be observed in the absence of an electrode reaction, (i.e. when  $i = 0$ ). This should be approximated by the value of  $I_{SER}$  at the foot of the voltammetric wave, where  $C_s \approx C_b$ . Consequently, the comparison between the potential dependence of  $I_{SER}$  and the corresponding current-potential curves in terms of Eq. (2) should provide useful insight into the relative redox reactivities of molecules at SERS-active and -inactive sites.

### Experimental

The rotating silver electrode had a disk radius of 0.2 cm, surrounded by a teflon sheath of radius 0.6 cm. The electrode was mechanically polished on a wheel successively with 5, 1, and 0.3  $\mu$ m alumina immediately prior to use. A compact electrode rotator of in-house design was utilized, featuring a photodiode speed controller. The cell was of conventional design, with a window at the base through which the krypton laser beam (647.1 nm, 100-300 mW power) focussed on the electrode surface. The cell was tilted so that the scattered light could be collected at 90° to the incident beam and about 60° to the electrode surface using a SPEX Triplemate/PAR OMA-2 photodiode array detector system. This enabled sequential Raman spectra to be recorded rapidly, each being obtained by signal accumulation for 1-5 seconds so to yield suitably large signal-to-noise ratios ( $\geq 5-10$ ) at the peak frequencies for the relevant SER bands. Simultaneous SERS- and rotating disk current-potential data could easily be obtained throughout the voltammetric wave within a time-scale (30-60 seconds) where the faradaic currents were reproducible and essentially no laser photolysis occurred.

Further electrochemical and chemical details for the systems studied here are given elsewhere.<sup>8-13</sup> Representative spectra are given in refs. 7 and 8. All electrode potentials are quoted versus the saturated calomel electrode (s.c.e.).

## Results and Discussion

Three model reactions were examined in this study. The first involves the one-electron reduction of hexaamminecobalt(III) at silver. This reaction is totally irreversible since the Co(II) product rapidly aquates to yield  $\text{Co}(\text{OH}_2)_6^{2+}$  which cannot reoxidize except at extreme positive potentials.<sup>13</sup> The electroreduction mechanism is expected to be outer-sphere since  $\text{Co}(\text{NH}_3)_6^{3+}$  is substitutionally inert and lacks ligands capable of binding to the electrode surface. Indeed, after double-layer corrections its electroreduction kinetics are essentially independent of the electrode material.<sup>11,12</sup> In perchlorate or hexafluorophosphate electrolytes at silver, well-defined rotating disk voltammograms are obtained with half-wave potentials,  $E_{1/2}$ , around -400 to -450 mV. Not surprisingly, no SER signals for  $\text{Co}(\text{NH}_3)_6^{3+}$  were detected using these electrolytes.

However, the addition of even small concentrations of chloride to acidified 0.1 M  $\text{NaClO}_4$  produced sizable positive shifts in  $E_{1/2}$  for  $\text{Co}(\text{NH}_3)_6^{3+}$  reduction. No further changes were seen for chloride concentrations above ca 0.5 mM; the  $E_{1/2}$  shift (ca 300 mV) corresponding to rate increases at a given potential of around  $10^4$ .<sup>14</sup> This catalytic influence of chloride can be accounted for quantitatively by the enhancement of the  $\text{Co}(\text{NH}_3)_6^{3+}$  concentration at the outer Helmholtz plane (o.H.p.) caused by chloride specific adsorption.<sup>15</sup> Most significantly for the present purpose, easily detectable SER spectra are obtained for  $\text{Co}(\text{NH}_3)_6^{3+}$  under these conditions.<sup>7</sup> Spectral bands observed include the symmetric N-H stretch at  $3200\text{ cm}^{-1}$ , and the  $A_{1g}$  and  $E_g$  Co-N stretching modes at 515 and  $450\text{ cm}^{-1}$ .<sup>7</sup> (Some mild roughening of the silver via an oxidation-reduction cycle in chloride media<sup>5</sup> is necessary to optimize the Raman

signal intensity. This has little effect on the electrochemical, including kinetic, properties of the surface beyond that resulting from a ca 1.5-2 fold increase in the microscopic electrode area.<sup>4)</sup>

Figure 1 contains plots (dashed curves) of the relative integrated intensity of the  $A_{1g}$  mode,  $I_{SER}$ , against the electrode potential for a pair of rotation speeds, 800 and 1600 r.p.m. The solution contained 1 mM  $Co(NH_3)_6^{3+}$  in 0.1 M  $NaClO_4$  + 0.01 M  $NaCl$ , with 2 mM  $HClO_4$  to avoid hydrolysis of the Co(II) product. The values of  $I_{SER}$  at the least negative potentials (+50 to -100 mV) are normalized to the values of  $i_l$  at these two rotation speeds; the corresponding  $i$ -E curves are also shown (solid curves) in Fig. 1. (In actuality, the values of  $I_{SER}$  in the region +50 to -100 mV are independent of rotation speed.) Comparison of the corresponding  $I_{SER}$ -E and  $i$ -E curves reveals that somewhat different behavior is encountered than that predicted by Eq. (2) in that the decreases in  $I_{SER}$  only commence at potentials close to the top of the voltammetric wave, where  $i \geq 0.9 i_l$  (Fig. 1). For example, according to Eq. (2),  $I_{SER}$  should equal  $0.5 I_{SER}^\circ$  at  $i = 0.5 i_l$  (i.e. at  $E_{1/2}$ ), whereas in actuality  $I_{SER} \approx I_{SER}^\circ$  at that point.

This apparent discrepancy can nonetheless be reconciled by noting that at potentials where  $I_{SER} \approx I_{SER}^\circ$  ( $\geq -110$  mV), the current is virtually independent of rotation speed, even though a sizable variation in  $C_s$  is expected on the basis of Eq. (1). Since it is expected that the current will be proportional to  $\Gamma_s$  at a given electrode potential, this result suggests that  $\Gamma_s$  is virtually independent of, rather than proportional to,  $C_s$  as is assumed in the derivation of Eq. (2). (In other words, the apparent reaction order,  $x$ , approaches zero, rather than equalling unity as expected under Henry's Law conditions.<sup>12</sup> Values

of  $x$  in the region ca 0.1-0.3 are obtained from an analysis of the dependence of the voltammograms upon rotation speed from 400-2,500 r.p.m.) This is consistent with values of  $\Gamma_s$  for  $\text{Co}(\text{NH}_3)_6^{3+}$  that are sufficiently large so as to approach saturation ( $\Gamma_s \sim 10^{-10} \text{ mol cm}^{-2}$ ), thereby accounting both for the large catalyses seen upon adding chloride and the appearance of the SERS signals. (Note that the reaction rate, and hence  $i$ , will be proportional to  $\Gamma_s$ .) Indeed, values of  $\Gamma_s$  approaching saturation (ca  $2 \times 10^{-11} \text{ mol cm}^{-2}$ ) are determined directly from rapid scan cyclic voltammetry for  $\text{Co}(\text{NH}_3)_6^{3+}$  and  $\text{Ru}(\text{NH}_3)_6^{3+}$  at silver in chloride-containing media, even for very small values of  $C_s$  (0.05 mM).<sup>7</sup> Consequently,  $\Gamma_s$  should remain virtually constant at values approaching saturation until  $C_s \ll C_b$ , corresponding to  $i \geq 0.9 i_l$  [Eq. (1)]. The observation that  $I_{\text{SER}}$  only decreases around this point close to the top of the voltammetric wave is therefore wholly consistent with the electrochemical behavior. This therefore suggests that the reaction energetics for  $\text{Co}(\text{NH}_3)_6^{3+}$  at the SERS-active sites do not differ noticeably from those at the sites predominantly responsible for the overall reaction rate.

The second reaction studied,  $\text{Cr}(\text{NH}_3)_5\text{Br}^{2+}$  reduction, was chosen since, unlike  $\text{Co}(\text{NH}_3)_6^{3+}$  reduction, it proceeds at silver via a well-defined inner-sphere pathway where the bromide ligand binds the reactant directly to the metal surface.<sup>9</sup> Diagnostic criteria supporting this mechanism include the rate decreases observed for  $\text{Cr}(\text{NH}_3)_5\text{Br}^{2+}$  reduction at silver upon the addition of chloride anions.<sup>9</sup> This contrasts the large rate increases noted above for  $\text{Co}(\text{NH}_3)_6^{3+}$  reduction and other outer-sphere reactions.<sup>9,12</sup> A metal-amine stretching mode,  $\nu_{\text{MN}}$ , is observed ( $450 \text{ cm}^{-1}$ ) in the SER spectra for  $\text{Cr}(\text{NH}_3)_5\text{Br}^{2+}$  in perchlorate media, along with a surface-bromide stretching mode at  $160 \text{ cm}^{-1}$ , thereby confirming the mode of attachment to the silver surface.<sup>7</sup> Similar to

$\text{Co}(\text{NH}_3)_6^{3+}$ , the reduction of  $\text{Cr}(\text{NH}_3)_5\text{Br}^{2+}$  is irreversible due to the lability of  $\text{Cr}(\text{II})$ , leading to a loss of the  $\nu_{\text{MN}}$  band. Reoxidation of  $\text{Cr}(\text{II})$  only occurs at potentials well positive of those for  $\text{Cr}(\text{NH}_3)_5\text{Br}^{2+}$  reduction, and therefore does not influence the cathodic voltammogram.

Figure 2 shows a typical plot of  $I_{\text{SER}}$  of the  $\nu_{\text{MN}}$  band for adsorbed  $\text{Cr}(\text{NH}_3)_5\text{Br}^{2+}$  against electrode potential (dashed curve) at a rotation speed of 800 r.p.m., along with the simultaneously recorded voltammogram (solid curve). As in Fig. 1, the  $I_{\text{SER}}$ -E and i-E curves are normalized to one another. Both the SER spectra and the reduction currents on the rising part of the wave were somewhat time dependent; smaller values of i and  $I_{\text{SER}}$  were obtained when returning from more negative potentials. The data in Fig. 2 are an average of several runs. Nevertheless, the results stand in sharp contrast to those in Fig. 1 in that  $I_{\text{SER}}$  drops sharply to zero at potentials close to the foot of the wave, where  $i/i_1 \leq 0.3$ .

These results are clearly at variance with the predictions of Eq. (2), in the opposite direction to those for  $\text{Co}(\text{NH}_3)_6^{3+}$  reduction. In contrast to the latter, the former cannot be rationalized on the basis of fractional electrochemical reaction orders since this only increases the discrepancies between the SERS and electrochemical data. Indeed apparent reaction orders somewhat below unity (ca 0.5-1) were obtained for  $\text{Cr}(\text{NH}_3)_5\text{Br}^{2+}$  reduction. The  $I_{\text{SER}}$ -E data for  $\text{Cr}(\text{NH}_3)_5\text{Br}^{2+}$  reduction therefore suggest that the adsorbate present at the SERS-active sites is reduced at noticeably smaller overpotentials, i.e. has a greater reactivity, than the prevalent adsorbate which is responsible for the i-E curves.

In order to examine this matter further, we undertook a similar comparison for  $\text{Cr}(\text{NH}_3)_5\text{NCS}^{2+}$  reduction. Like  $\text{Cr}(\text{NH}_3)_5\text{Br}^{2+}$  reduction, this reaction proceeds via an irreversible inner-sphere mechanism since the remote thiocyanate sulfur binds strongly to the silver surface.<sup>9</sup> The SERS  $\nu_{\text{CN}}$  mode for  $\text{Cr}(\text{NH}_3)_5\text{NCS}^{2+}$  ( $450\text{ cm}^{-1}$ ) is rather weak, making it unsuitable for monitoring the adsorbate concentration. Nevertheless, the C-N stretching mode,  $\nu_{\text{CN}}$ , is suitably intense for this purpose. Although the thiocyanate ligand released upon formation of Cr(II) is also adsorbed and exhibits a SERS  $\nu_{\text{CN}}$  band, its intensity is ca 5 to 10-fold weaker, and occurs at frequencies about  $20\text{ cm}^{-1}$  lower than  $\nu_{\text{CN}}$  for adsorbed  $\text{Cr}(\text{NH}_3)_5\text{NCS}^{2+}$  at the potentials (ca -600 mV) where  $\text{Cr}(\text{NH}_3)_5\text{NCS}^{2+}$  reduction commences.<sup>8</sup> Consequently, the reduction of adsorbed  $\text{Cr}(\text{NH}_3)_5\text{NCS}^{2+}$  can be followed either from the intensity decreases, or from the decreases in the peak frequency of the  $\nu_{\text{CN}}$  band.

Figure 3 contains a plot of the integrated intensity of the  $\nu_{\text{CN}}$  band,  $I_{\text{SER}}$ , against electrode potential (dashed line) along with the corresponding voltammogram at 800 r.p.m. (solid curve) for  $\text{Cr}(\text{NH}_3)_5\text{NCS}^{2+}$  reduction (c.f. Figs. 1, 2). Similar to  $\text{Cr}(\text{NH}_3)_5\text{Br}^{2+}$  reduction, the SER signal for adsorbed Cr(III) is almost entirely lost at the foot of the voltammetric wave, i.e. for  $i/i_1 \leq 0.2$ . It might be argued that this decrease in  $I_{\text{SER}}$  results from a potential dependence of the surface Raman scattering efficiency or from reactant desorption rather than from reduction of  $\text{Cr}(\text{NH}_3)_5\text{NCS}^{2+}$ . Indeed  $I_{\text{SER}}$  is somewhat potential-dependent in the region well positive of the voltammetric wave (Fig. 3) as in  $I_{\text{SER}}$  for  $\text{Cr}(\text{NH}_3)_5\text{Br}^{2+}$  (Fig. 2). However, strong evidence against these possibilities is provided by the corresponding plot of the peak frequency,  $\nu_{\text{CN}}$ , against electrode potential (the dotted-dashed curve in Fig. 3). Thus the sharp decrease in  $I_{\text{SER}}$  over the potential region -500 to -600 mV coincides with a marked change

in  $\nu_{\text{CN}}$  from 2125 to 2090  $\text{cm}^{-1}$ , consistent with complete reduction of adsorbed  $\text{Cr}(\text{NH}_3)_5\text{NCS}^{2+}$  to form  $\text{NCS}^-$ .<sup>8</sup> This result is especially striking since apparent reaction orders approaching zero ( $\leq 0.3$ ) are obtained from the rotation speed-dependent voltammograms for  $\text{Cr}(\text{NH}_3)_5\text{NCS}^{2+}$  reduction at silver.<sup>9</sup> As for  $\text{Co}(\text{NH}_3)_6^{3+}$  above, such fractional reaction orders are consistent with adsorbed reactant coverages that approach a monolayer, as is indeed found ( $\Gamma_s \sim 2 \times 10^{-10} \text{ mol cm}^{-2}$ ) from rapid cyclic voltammetry.<sup>9,10</sup> On the basis of the arguments presented above, the  $I_{\text{SER}}$ -E and i-E curves for  $\text{Cr}(\text{NH}_3)_5\text{NCS}^{2+}$  reduction also differ very markedly with the prediction of Eq. (2).

Rotating-disk voltammograms were recorded both in the absence and presence of laser illumination. Although virtually identical voltammograms were obtained, small additional cathodic currents ( $\sim 20 \text{ } \mu\text{A cm}^{-2}$ ) were detected during laser irradiation. These photocurrents are only mildly dependent on the electrode potential, and were observed even at potentials well positive of the rising part of the voltammograms, i.e. where potential-independent SERS intensities are obtained and the thermal electroreduction currents are undetectably small. The photocurrents are only observed in the presence of high reactant surface concentrations. The possibility that the effect is due to enhancement of the thermal electrochemical kinetics by surface laser heating was considered. However, this was eliminated both on the basis of the above evidence and model calculations (as described in ref. 16) which indicate that the laser-induced temperature rise at the silver surface was negligible ( $\leq 1^\circ\text{C}$ ) under the conditions employed. Further study of the effect has led us to identify it tentatively as photoemission involving photoreduction of the adsorbed reactant. Details will be given elsewhere.<sup>17</sup> For the present purposes, it is important to note that the photocurrents do not appear to be connected with either the electroreduction pathways

as monitored by the rotating-disk voltammetry, or with the potential dependence of the SERS intensities.

The present results therefore indicate that both  $\text{Cr}(\text{NH}_3)_5\text{Br}^{2+}$  and  $\text{Cr}(\text{NH}_3)_5\text{NCS}^{2+}$  adsorbed at SERS-active sites undergo noticeably more facile electroreduction than the majority of the adsorbate. This finding contrasts that obtained for the outer-sphere reduction of  $\text{Co}(\text{NH}_3)_6^{3+}$  where the SERS-active species display reactivities more representative of the overall surface. Therefore such reactants bound directly to SERS-active sites are perturbed energetically in a manner which is not observed for unbound reactant. This is consistent with the observation that linear sweep voltammograms for reduction of adsorbed  $\text{Cr}(\text{NH}_3)_5\text{NCS}^{2+}$  and related complexes at silver yield unexpectedly broad reduction peaks.<sup>9,10,16</sup> A typical such voltammogram is shown in Fig. 4 (solid curve); under the conditions chosen (sweep rate =  $50 \text{ v sec}^{-1}$ , reactant concentration =  $50 \text{ }\mu\text{M}$ ) the current for  $\text{Cr}(\text{NH}_3)_5\text{NCS}^{2+}$  reduction arising from diffusing reactant can be neglected. Very similar voltammograms were obtained for smooth electropolished and electrochemically roughened (i.e. SERS-active) electrodes, save from the ca 1.5 to 2 fold higher currents for the latter associated with the larger effective electrode area. Although the cathodic reduction peak is somewhat ill-defined, it is substantially broader than that expected (half-peak width ca  $125 \text{ mV}$ .<sup>19</sup>) for a surface where all the adsorption sites are energetically equivalent.

This result, which is typically obtained for adsorbed  $\text{Cr}(\text{III})$  and  $\text{Co}(\text{III})$  reactants at polycrystalline surfaces<sup>9,10</sup> but not at mercury,<sup>9,18</sup> suggests that a polycrystalline metal provides a number of surface binding sites with significantly different electrocatalytic properties. Presumably the currents at the foot of the steady-state voltammetric waves in Figs. 2 and 3 are associated with reduction of adsorbate at the most catalytic sites

which also contribute predominantly to the SERS signals. In this regard it is interesting to note that the cyclic voltammetric reduction wave for adsorbed  $\text{Cr}(\text{NH}_3)_5\text{NCS}^{2+}$  (Fig. 4) also commences beyond -600 mV, although comparison with the steady-state voltammetric currents in Fig. 3 is difficult given the different solution conditions. The occurrence of such "active sites" for the present ligand-bridged reactions requires that the unimolecular rate constants for the adsorbed reactants are sensitive to the substrate structure. Such a dependence is indeed indicated from experimental data.<sup>9</sup> Although it is difficult to estimate the fraction of the overall adsorbed reactant bound to such SERS-active sites, on the basis of the present evidence it is liable to be small, probably less than 5%.

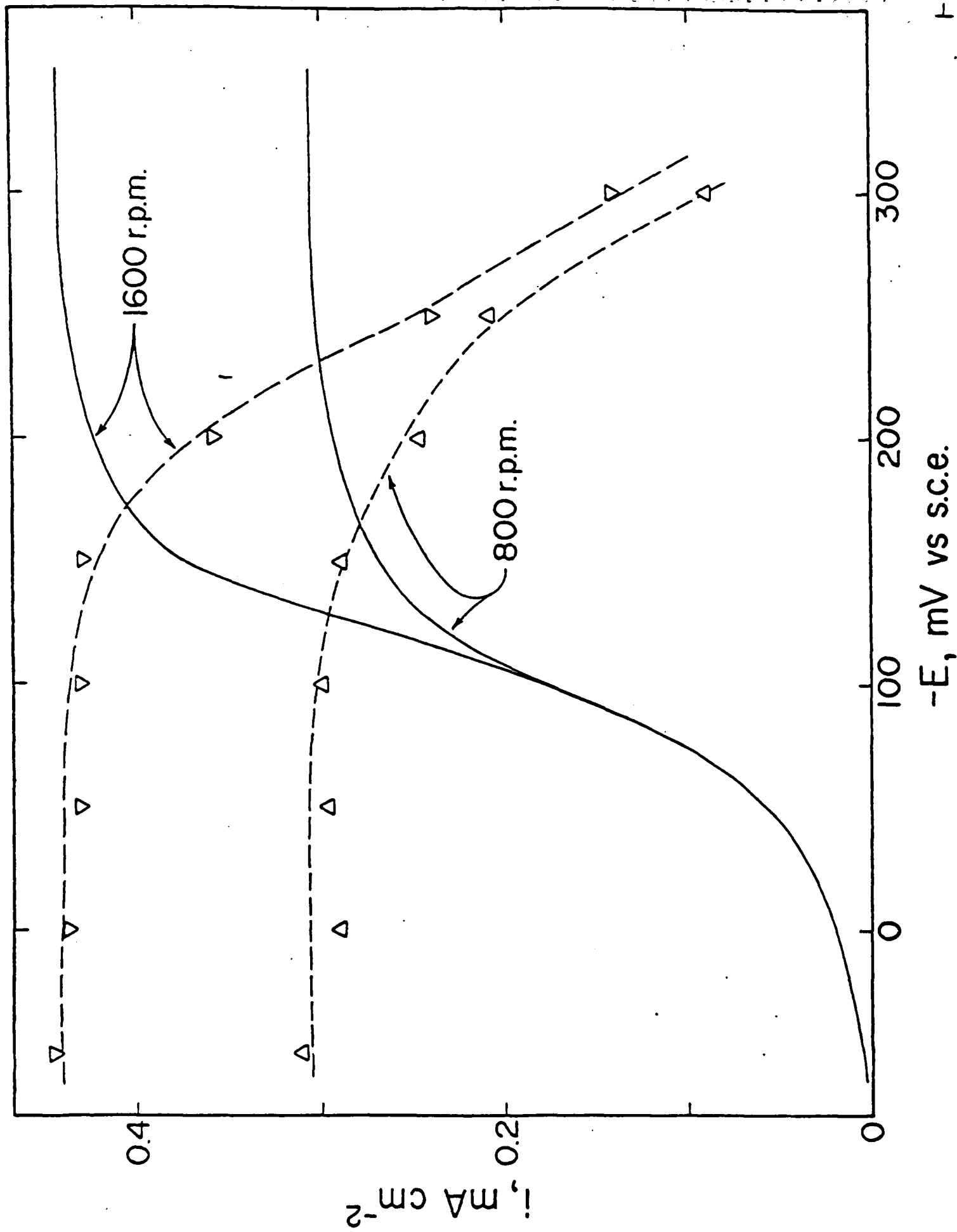
The observed electrocatalytic potency of the SERS-active sites is not entirely unexpected given the likelihood that particular surface morphologies, such as surface metal defects or clusters, contribute importantly to SERS.<sup>1,2</sup> Such sites should bind strongly to incoming reactant, and are anticipated to yield especially large unimolecular rate constants and therefore enhanced overall reactivities for inner-sphere electron transfer,<sup>9</sup> as observed. Whether or not these results portend well for the applicability of SERS to surface reaction dynamics is a somewhat subjective issue at this point. Regardless, the utilization of rapid photodiode array detectors to gather time-resolved SER spectra in conjunction with transient kinetic experiments should yield fresh perspectives into the molecular basis of heterogeneous catalysis.

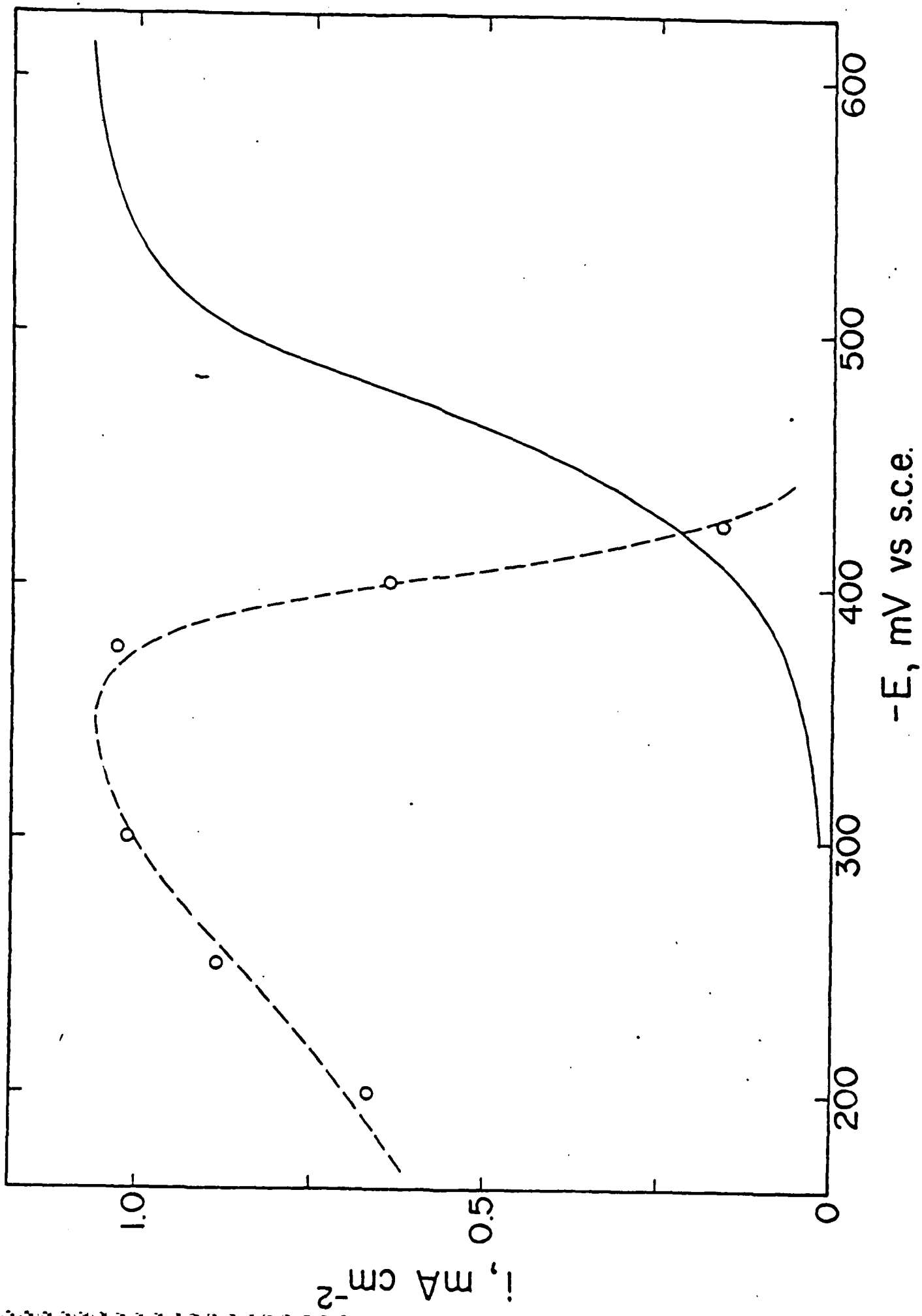
Acknowledgments

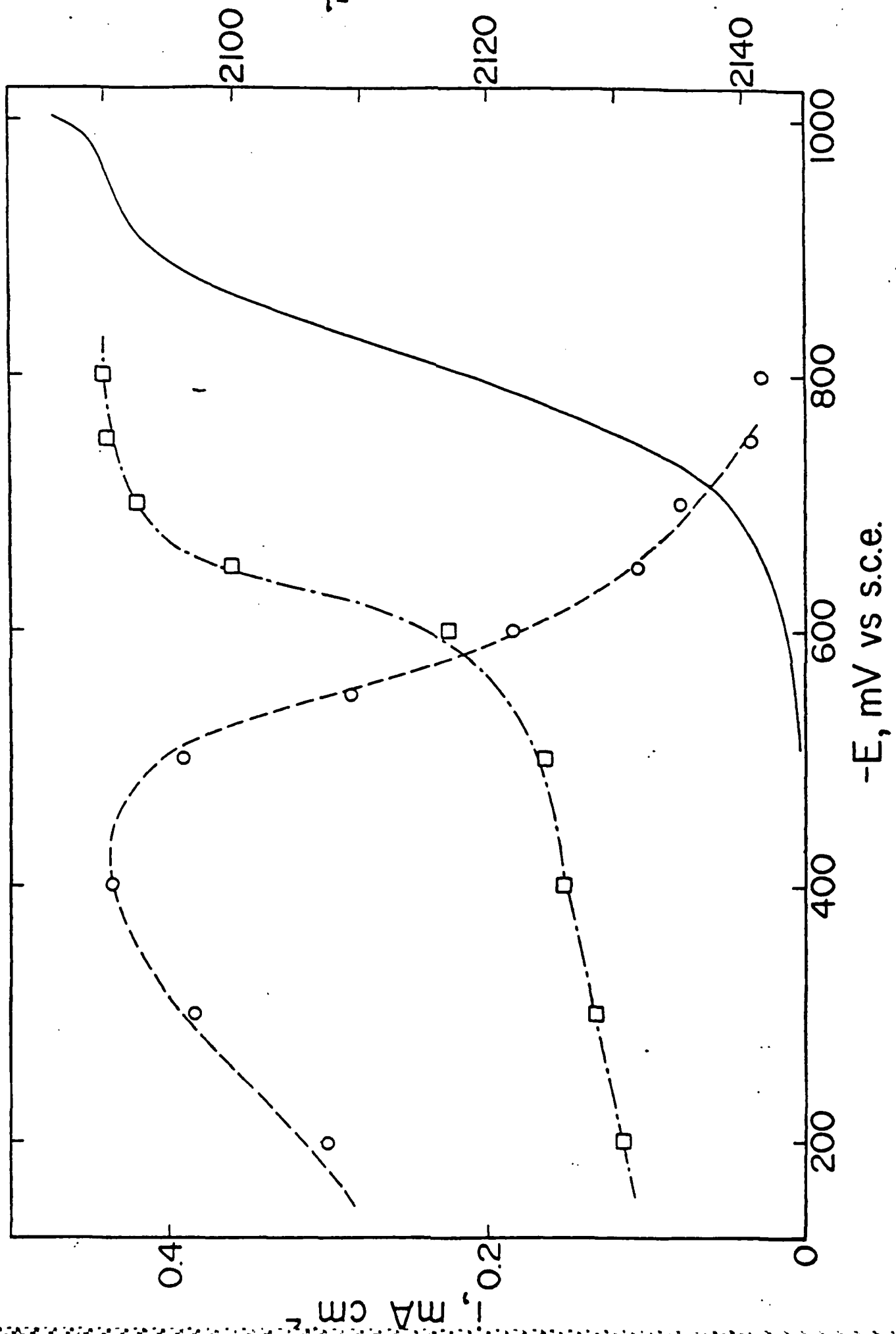
Careful electrochemical measurements undertaken by Ken Guyer provided an invaluable background for the present study. This work is supported in part by the Office of Naval Research, the Air Force Office of Scientific Research, and the NSF Materials Research Laboratory at Purdue. M.J.W. acknowledges a fellowship from the Alfred P. Sloan Foundation.

# References

1. For recent reviews, (a) T. E. Furtak, J. Reyes, Surf. Sci. 93 (1980), 351; (b) R. L. Burke, J. R. Lombardi, L. A. Sanchez, Adv. Chem. Ser. 201 (1982), 69; (c) R. K. Chang, T. E. Furtak (eds), "Surface Enhanced Raman Scattering", Plenum, New York, 1982; (d) A. Otto, in Light Scattering in Solids", M. Cardona, G. Guntherodt (eds), Springer, Berlin, 1984; (e) R. K. Chang, B. L. Laube, CRC Crit. Rev. Solid State Mat. Sci., in press.
2. For example, see W. J. Pleith, J. Phys. Chem. 86 (1982), 3166; T. Watanabe, O. Kawanami, K. Houda, B. Pettinger, Chem. Phys. Lett. 102 (1983), 565.
3. M. J. Weaver, F. Barz, J. G. Gordon II, M. R. Philpott, Surf. Sci. 125 (1983), 409.
4. J. T. Hupp, D. Larkin, M. J. Weaver, Surf. Sci. 125 (1983), 429.
5. M. J. Weaver, J. T. Hupp, F. Barz, J. G. Gordon II, M. R. Philpott, J. Electroanal. Chem., in press.
6. S. Farquharson, M. J. Weaver, P. A. Lay, R. H. Magnuson, H. Taube, J. Am. Chem. Soc. 105 (1983), 3350; S. Farquharson, K. L. Guyer, P. A. Lay, R. H. Magnuson, M. J. Weaver, J. Am. Chem. Soc., in press.
7. M. A. Tadayyoni, S. Farquharson, M. J. Weaver, J. Chem. Phys., 80 (1984), 1363.
8. M. A. Tadayyoni, S. Farquharson, T. T-T. Li, M. J. Weaver, J. Phys. Chem., in press.
9. K. L. Guyer, M. J. Weaver, Inorg. Chem., in press.
10. K. L. Guyer, S. W. Barr, M. J. Weaver, "Proc. Symp. on Electrocatalysis", W. E. O'Grady, P. N. Ross, Jr., F. G. Wills (eds), Electrochemical Society, Pennington, N.J., 1982, p. 377.
11. S. W. Barr, K. L. Guyer, M. J. Weaver, J. Electroanal. Chem. 111 (1980), 41.
12. K. L. Guyer, S. W. Barr, R. J. Cave, M. J. Weaver, in "Proc. 3rd Symp. on Electrode Processes", S. Bruckenstein, J. D. E. McIntyre, B. Miller, E. Yeager (eds), Electrochemical Society, Pennington, N.J., 1980, p. 390.
13. T. L. Satterberg, M. J. Weaver, J. Phys. Chem. 82 (1978), 1784.
14. K. L. Guyer, unpublished results.
15. D. Larkin, K. L. Guyer, J. T. Hupp, M. J. Weaver, J. Electroanal. Chem. 138 (1982), 401.
16. J. F. Ready, "Effects of High Power Laser Radiation", Academic Press, New York, 1971, Chapter 3.
17. D. Corrigan, M. J. Weaver, to be published.
18. T. T-T. Li, H. Y. Liu, M. J. Weaver, J. Am. Chem. Soc., 106 (1984), 1233.
19. See for example, A. J. Bard, L. R. Faulkner, "Electrochemical Methods", Wiley, New York, 1980, p. 525.







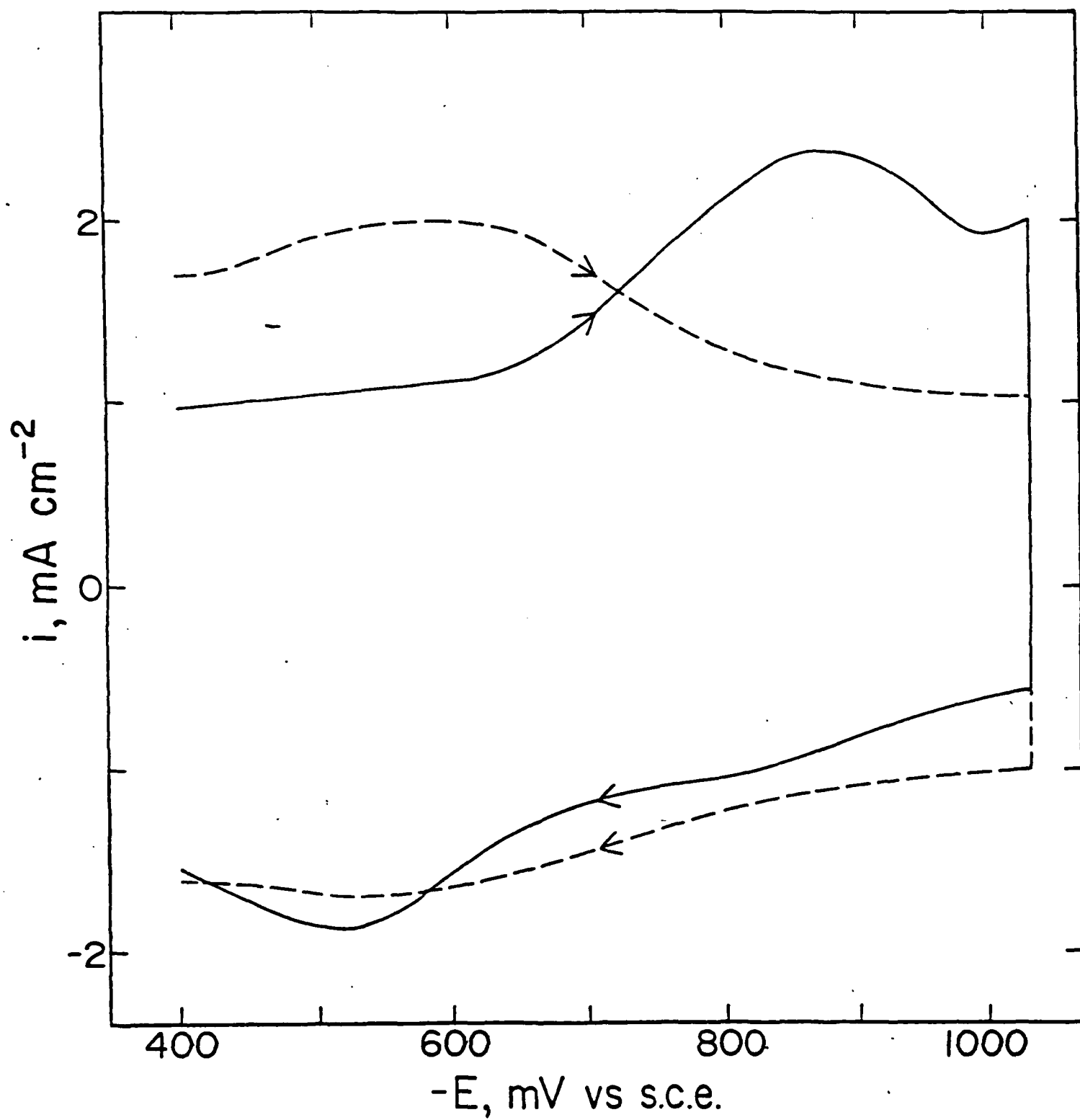


### Figure Captions

Figure 1 Plots of current density,  $i$ , for  $\text{Co}(\text{NH}_3)_6^{3+}$  reduction at a rotating silver electrode against electrode potential,  $E$ , (solid curves) compared with corresponding plots of integrated intensity,  $I_{\text{SER}}$ , of SERS  $\text{Co}^{\text{III}}\text{-NH}_3$  stretching mode ( $515\text{ cm}^{-1}$ ) against  $E$  (dashed curves). Solution contained  $1\text{ mM Co}(\text{NH}_3)_6^{3+}$  in  $0.1\text{ M NaClO}_4 + 0.01\text{ M NaCl} + 2\text{ mM HClO}_4$ . Lower curves:  $800\text{ r.p.m.}$ ; Upper curves:  $1600\text{ r.p.m.}$  rotation speed. Maximum values of  $I_{\text{SER}}$  (arbitrary scale) set equal to maximum values of  $i$  at the same rotation speed. Uncertainties in  $I_{\text{SER}}$  values typically less than 5-10%.

Figure 2 Plot of current density,  $i$ , for  $\text{Cr}(\text{NH}_3)_5\text{Br}^{2+}$  reduction against electrode potential,  $E$  (solid curve), in comparison with integrated intensity,  $I_{\text{SER}}$ , of SERS  $\text{Cr}^{\text{III}}\text{-NH}_3$  stretching mode ( $450\text{ cm}^{-1}$ ) against  $E$  (dashed curve). Solution contained  $3\text{ mM Cr}(\text{NH}_3)_5\text{Br}^{2+}$  in  $0.1\text{ M NaClO}_4 + 5\text{ mM NaCl} + 2\text{ mM HClO}_4$ . Silver electrode was rotated at  $800\text{ r.p.m.}$  Maximum value of  $I_{\text{SER}}$  set equal to maximum value of  $i$ .

Figure 3 Plot of current density,  $i$ , for  $\text{Cr}(\text{NH}_3)_5\text{NCS}^{2+}$  reduction against electrode potential,  $E$  (solid curve), in comparison with integrated intensity,  $I_{\text{SER}}$ , of SERS C-N stretching mode ( $2090 - 2130\text{ cm}^{-1}$ ) against  $E$  (dashed curve). Solution contained  $1.2\text{ mM Cr}(\text{NH}_3)_5\text{NCS}^{2+}$  in  $0.1\text{ M NaClO}_4 + 5\text{ mM NaCl} + 2\text{ mM HClO}_4$ . Silver electrode was rotated at  $800\text{ r.p.m.}$  Maximum value of  $I_{\text{SER}}$  set equal to maximum value of  $i$ . Dotted-dashed curve is corresponding plot of peak frequency of C-N stretching mode,  $\nu_{\text{CN}}$ , (right-hand y axis) against electrode potential.

Figure 4 Cathodic-anodic cyclic voltammogram (solid curves) for reduction of adsorbed  $\text{Cr}(\text{NH}_3)_5\text{NCS}^{2+}$  at silver electrode. Electrolyte conditions as in Fig. 3 except that  $\text{Cr}(\text{NH}_3)_5\text{NCS}^{2+}$  concentration was 50  $\mu\text{M}$ ; electrode was electropolished as in ref. 15. Sweep rate was 50  $\text{V sec}^{-1}$ . Dashed curve is corresponding voltammogram obtained in absence of adsorbed reactant.